



Published in final edited form as:

IEEE Trans Biomed Eng. 2009 January ; 56(1): 65–73. doi:10.1109/TBME.2008.2003293.

A Strategy for Identifying Locomotion Modes Using Surface Electromyography

He Huang[Member, IEEE],

Department of Electrical, Computer, and Biomedical Engineering, University of Rhode Island, Kingston, RI 02881 USA

Todd A. Kuiken[Senior Member, IEEE], and

Neural Engineering Center for Artificial Limbs, Rehabilitation Institute of Chicago, Chicago, IL 60611 USA, and also with the Department of Physical Medicine and Rehabilitation, and the Department of Biomedical Engineering, Northwestern University, Chicago, IL 60611 USA

Robert D. Lipschutz

Neural Engineering Center for Artificial Limbs, Rehabilitation Institute of Chicago, Chicago, IL 60611 USA

He Huang: huang@ele.uri.edu

Abstract

This study investigated the use of surface electromyography (EMG) combined with pattern recognition (PR) to identify user locomotion modes. Due to the nonstationary characteristics of leg EMG signals during locomotion, a new phase-dependent EMG PR strategy was proposed for classifying the user's locomotion modes. The variables of the system were studied for accurate classification and timely system response. The developed PR system was tested on EMG data collected from eight able-bodied subjects and two subjects with long transfemoral (TF) amputations while they were walking on different terrains or paths. The results showed reliable classification for the seven tested modes. For eight able-bodied subjects, the average classification errors in the four defined phases using ten electrodes located over the muscles above the knee (simulating EMG from the residual limb of a TF amputee) were $12.4\% \pm 5.0\%$, $6.0\% \pm 4.7\%$, $7.5\% \pm 5.1\%$, and $5.2\% \pm 3.7\%$, respectively. Comparable results were also observed in our pilot study on the subjects with TF amputations. The outcome of this investigation could promote the future design of neural-controlled artificial legs.

Index Terms

Electromyography (EMG); neural-machine interface; pattern recognition (PR); prosthesis; targeted muscle reinnervation

I. Introduction

Recent designs of lower limb prostheses have offered amputee patients improved stability and some decrease in energy consumption in level-ground walking [1], [2]. In addition, advances in computerized control and powered prosthesis design have further improved the function of artificial legs; these legs can assist users with versatile activities beyond level walking. However, without knowing user movement intent, the artificial limb cannot

properly select the correct control mode to adjust the joint impedance [3], [4] or drive powered joint motion. Current computerized prosthetic legs allow the user to change the movement mode manually [1]. Such voluntary prosthesis control is cumbersome and does not allow smooth task transition. Therefore, neural control of computerized, powered prosthetic legs is demanded.

Surface electromyographic (EMG) signals are one of the major neural control sources for powered upper limb prostheses, experimental motorized orthoses, and rehabilitation robots. Although myoelectric control and advanced EMG pattern recognition (PR)-based control have been used in upper limb prostheses for decades [5]–[8], no EMG-controlled lower limb prostheses are commercially available, and published studies in this area are limited [9], [10]. Recently, the need for neural control of prosthetic legs has brought the idea of EMG-based control back to attention. Two previous studies have attempted to use EMG signals to identify locomotion modes for prosthetic leg control [3], [11], but they lacked systematic experimental design and study methodology. Peeraer *et al.* [3] demonstrated the difference in the EMG signal envelope among level-ground walking, and ascending and descending a ramp; they concluded that EMG signals from hip muscles might be used to classify these locomotion modes. However, no method or result was reported. Jin *et al.* [11] developed an algorithm for terrain identification during walking. The features were extracted from EMG signals from a complete stride cycle. Using such features, the algorithm only made one decision per stride cycle, resulting in a time delay of one stride cycle in real time. In practical application, this is inadequate for safe prosthetic control. Therefore, a strategy is needed to generate timely updates of the user's lower limb movement modes.

One of the challenges in using EMG signals from leg muscles to classify the users' movement modes in a timely manner is that the recorded EMG signals are time-varying. The features of gait EMG signals generally show large variation within the same task mode (class), which might result in overlaps of features among classes, and therefore, low accuracy for PR. Some related work in upper limb prosthesis control does give encouragement. Hudgins *et al.* [7] used 200-ms transient EMG signals, which were nonstationary, at the onset of muscle activation to classify four movements; they obtained 90% classification accuracy. This result implies that the EMG signals, though time-varying, had a relatively small change in signal content within the short time duration of 200 ms. The EMG PR algorithms developed for stationary EMG recordings, such as those for upper limb prosthesis control, might be used for short-time, nonstationary EMG recordings.

Another challenge is that the accuracy of EMG PR might be inadequate for robust prosthesis control in patients with high-level amputations if insufficient neural content is available in EMG signals from the residual limb. However, the neural control information for an amputated limb remains in the residual nerves. To allow access to this information via EMG signals, a novel neural-machine interface called targeted muscle reinnervation (TMR) has been developed and successfully applied on patients with transhumeral or higher amputations for improved myoelectric artificial arm control [12], [13]. In TMR surgery, the residual nerves are transferred to alternative muscles that are no longer biomechanically functional. After successful motor reinnervation, the voluntary neural control signals propagate along the efferent nerves and activate these muscles. The resultant EMG signals, containing neural control information for the missing arm and hand, can control an artificial elbow, wrist, and even thumb and fingers via an EMG PR method [14], [15]. We hypothesize that TMR could be used for leg prosthesis control in that it could provide control information for the lower leg and foot in the form of EMG signals from reinnervated muscle. However, efforts are required to quantify the potential benefits of TMR before its clinical application to artificial leg control.

Motivated by the need for neural control of prosthetic legs, we investigated how accurately a variety of mobility tasks could be identified using nonstationary EMG signals recorded from leg muscles. A new EMG PR strategy was designed. EMG signals recorded from eight able-bodied subjects and two subjects with long transfemoral (TF) amputations were used to evaluate the potential of the designed EMG PR algorithm for neural control of artificial legs. Sufficient information for accurate task identification was extracted from the EMG signals recorded from gluteal and thigh muscles in eight able-bodied subjects and two amputee subjects. The outcome of this study will aid the future development of neural-controlled artificial legs for assisting lower limb amputees with versatile activities.

II. Methods

A. Participants and Measurements

This study was conducted with the Institutional Review Board (IRB) approval and the informed consent of all subjects. Four male and four female subjects, free from orthopedic or neurological pathologies, were recruited. The average age of the subjects was 41.3 (± 12.9) years; the average weight of the subjects was 65.8 (± 7.7) kg; the average height was 1.71 (± 0.05) m. Sixteen channels of surface EMG signals from muscles on one lower limb were collected. The monitored muscles included the *gluteus maximus* (GMA), *gluteus medius* (GME), *sartorius* (SAR), *rectus femoris* (RF), *vastus lateralis* (VL), *vastus medialis* (VM), *gracilis* (GRA), *biceps femoris long head* (BFL), *semitendinosus* (SEM), *biceps femoris short head* (BFS), *tibialis anterior* (TA), *peroneus longus* (PL), *gastrocnemius lateral head* (GASL), *gastrocnemius medial head* (GASM), *soleus* (SOL), and *extensor digitorum brevis* (EDB). The bipolar electrodes were placed over the anatomical locations described by Delagi and Perotto [16].

Since the design of an EMG-based neural-machine interface was motivated by the need for neural control of artificial legs, two male subjects (TF1 and TF2) with long, unilateral TF amputations were also recruited. They were 32 years and 38 years postamputation, respectively. The ratio between the length of residual limb (measured from the greater trochanter to the amputated site) to the thigh length on the nonimpaired side (measured from the greater trochanter to lateral epicondyle) was 0.82 for TF1 and 0.62 for TF2. Two gluteal muscles (GMA and GME) and nine residual thigh muscles, the SAR, RF, VL, VM, GRA, BFL, SEM, BFS, and *adductor magnus* (ADM), were monitored. It is noteworthy that the locations of EMG electrodes on the distal muscles were approximate.

Active surface EMG electrodes were used to record signals from all subjects. The electrodes contained a preamplifier that bandpass filtered the EMG signals between 20 and 3000 Hz with a passband gain of 20. For able-bodied subjects, the electrodes (MA-411, Motion Lab System, Inc., Baton Rouge, LA) had two circular sensor contacts (12 mm in diameter), between which was one rectangular reference contact to remove the electromagnetic environmental noise. The center-to-center separation of the two poles was 18 mm. For the amputee subjects, the electrodes (MA-411-002, Motion Lab System, Inc.) consisted of two contacts only, and were mounted on an experimental socket. The contacts of the electrodes were replaced with LTI (Liberating Technologies, Inc., Holliston, MA) electrode domes, which can penetrate the experimental socket for reliable electrode-skin contact. Before electrode placement or socket donning, the skin was shaved and cleaned. A ground electrode was placed on the bony area of the knee for able-bodied subjects and near the anterior iliac spine for amputee subjects.

Gait events were detected by force-sensitive-resistor-based footswitches placed under the tested foot and via motion data of light reflective markers placed over the heel and toe. An MA-300-16 system (Motion Lab System, Inc.) collected 16 channels of EMG data and

footswitch data simultaneously. The cutoff frequency of the antialiasing filter was 500 Hz for EMG channels and 120 Hz for footswitch data. Both sources were then digitally sampled at a rate of 1440 Hz. The markers' positions were captured by six motion-tracking cameras (Motion Analysis Corp., Santa Rosa, CA) and then sampled at 120 Hz. All recordings were synchronized.

B. Experiment Protocol

In the experiment, the able-bodied subjects wore their own walking shoes, and the TF subjects wore their own prostheses (a Mauch SNS knee and a 27-cm Vari-Flex foot for TF1; a Mauch SNS knee and a 28-cm Pathfinder foot for TF2). Experimental sockets were duplicated from their own ischial containment sockets with suction suspension. In addition, total elastic suspension belts were applied to reinforce the socket suspension. The subjects received instructions and practiced the tasks several times prior to measurement.

Seven movement modes were investigated: level-ground walking, stepping over an obstacle, ascending stairs, descending stairs, ipsilateral turning, contralateral turning, and standing still. Level walking was tested on a straight walkway 9 m in length. Subjects were instructed to walk at a comfortable speed. For the task of stepping over an obstacle, subjects were asked to step over a box (19 cm high \times 30 cm width \times 10 cm depth) during ambulation. For the able-bodied subjects, the nontesting side was required to pass over the obstacle first, followed by the instrumented leg. The amputee subjects were instructed to use their own preferences; they chose the amputated side as the leading limb. A three-stair staircase was used for stair ascent/descent tests. The staircase was 20 cm high, 75 cm wide, and 26 cm deep. TF1 was capable of performing stair ascent with the normal alternating pattern when using hand railings while TF2 ascended the stairs one step at a time. In the turning tasks, the subjects were instructed to perform 90° turns during locomotion. When the subject turned toward the tested leg, the task was called ipsilateral turning, otherwise the task was termed contralateral turning. Previous studies indicated two turning strategies, step turn and spin turn, depending on the side of the foot used as the pivot [17]. The turning strategy used by both the able-bodied subjects and the amputee subjects was the step turn strategy, which employed the contralateral limb as the pivot. Finally, EMG signals were recorded while the subjects were standing still.

In each trial, subjects performed one type of task. Each locomotion mode was repeated, and at least ten complete stride cycles of each task mode were recorded. The order of the tasks was randomly assigned. Rest periods were allowed between trials to avoid fatigue.

C. Data Analysis

1) Phase-Dependent Classifier—Conventional classifiers for upper limb prosthesis control may not correctly identify locomotion modes because of how leg EMG patterns change over time within the same mode [see Fig. 1(b)]. Fortunately, gait EMG signals, although time-varying, are quasi-cyclic; the muscles' activation patterns for the same locomotion mode are similar at the same gait phase. In addition, we assumed that the pattern of gait EMG signals had small variation in a short time window, and therefore, designed a phase-dependent EMG pattern classifier to recognize the user's locomotion modes with a fast time response [see Fig. 1(a)]. We hypothesized that the phase-dependent PR design could provide more reliable classification than a more conventional PR system, which uses EMG signals from an entire stride.

To test phase-dependent PR design concepts, four-phase windows aligned with two gait events, heel-contact (HC) and toe-off (TO), were defined [see Fig. 1(b)]. Specifically, they were the time windows: 1) immediately after HC (Post-HC); 2) prior to TO (Pre-TO); 3)

immediately after toe-off (Post-TO); and 4) prior to the next HC (Pre-HC). One classifier was built for each phase window. The phase detection module detected the gait events and switched on the associated classifier. At least one decision could be made in every gait phase window. Based on the study of Hudgins *et al.* [7], we defined the duration of each phase window, in which the EMG signals were assumed to be quasi-stationary, as 200 ms. It is noteworthy that data overlapping was observed between the Post-TO and Pre-HC phases for the tasks of level-ground walking and descending stairs. For level-ground walking, two able-bodied subjects with fast cadences showed an average of 38 and 4 ms of data overlapping separately; for the task of descending stairs, four able-bodied subjects had an average data overlapping ranging from 21 to 41 ms. The classification accuracy when using the phase-dependent PR system was compared to that when using PR composed of one classifier trained by EMG data from the entire stride cycle.

2) EMG PR—Raw EMG data were high-pass filtered with a 25-Hz cutoff frequency to remove motion artifacts. At least ten stride cycles were selected for each task. For example, stride cycles in the turning task were segmented starting at the HC before turning and ending at the next HC with changed foot orientation. For the stair-descent task, although the toe touched the staircase before the heel for able-bodied subjects, the cycles were picked based on the timing of heel contact. For the phase-dependent PR system, EMG data from the four defined phases were further sampled within each stride cycle.

In each defined phase, EMG features were computed in every analysis window. A feature vector (\bar{F}) was formulated as

$$\bar{F} = \{\bar{f}_1, \bar{f}_2, \bar{f}_3, \dots, \bar{f}_N\} \quad (1)$$

where \bar{f}_n denotes the EMG features of channel n and N denotes the total number of EMG channels. These vectors were then separated into a set to train the classifier (the training set) and a set to evaluate the classifier (the testing set). Due to the relatively small sample size, leave-one-out cross-validation (LOOCV) was used in each phase for more precise estimation of the classification error [18]. In the LOOCV procedure, data in one gait cycle of each movement mode were applied as the testing data; the features \bar{F} in the remaining cycles were used as the training data. This procedure was repeated so that each cycle in all recorded gait cycles was used once as the testing data. To quantify the performance of the classifier, the overall classification error (CE) was calculated by (2), following the LOOCV routine.

$$CE = \frac{\text{number of misclassified testing data}}{\text{total number of applied testing data}} \times 100\%. \quad (2)$$

Additionally, the confusion matrix (C) listing the test results between the targeted classes and the estimated task classes was computed.

$$C = \begin{bmatrix} a_{11} & a_{12} & \cdots & a_{17} \\ \cdots & a_{22} & \cdots & \cdots \\ \cdots & \cdots & \cdots & \cdots \\ a_{71} & \cdots & \cdots & a_{77} \end{bmatrix}_{7 \times 7} \quad (3)$$

where each element is defined as

$$a_{ij} = \frac{\text{number of testing data in class } i \text{ estimated as class } j}{\text{total number of testing data in targeted class } i} \times 100\%. \quad (4)$$

The diagonal of the confusion matrix a_{ij} is the classification accuracy of task class i . Other elements indicate the misclassification of EMG patterns between the targeted class i and the estimated class j ($i \neq j$). Note that for the able-bodied subjects, the averaged classification accuracy over task modes was slightly different from the overall classification accuracy because the number of sampled gait cycles between task modes varied slightly.

3) Influence of Design Parameters on Classifier Performance—To develop a robust, real-time EMG PR algorithm, we studied how the classification error (CE) was influenced by classifier types, EMG features, the length of the analysis window, and the analysis window increment size. Only the EMG data recorded from the able-bodied subjects were used.

a) Classifier: Comparable classification performance has been reported among different types of classifiers for myoelectric artificial arm control [19]–[22]. In the present study, we investigated a simple linear discriminant analysis (LDA) classifier and a more complex artificial neural network (ANN) classifier. The LDA and ANN classifiers are well-understood representatives of statistical and neural classifiers, respectively. They have been repeatedly used for EMG pattern classification and compared by their classification accuracies [7], [21]–[24]. The LDA treats each feature as an independent variable, while the ANN determines the class assignment by feature structures [24]. In addition, the ANN employs a recursive training procedure to generate nonlinear boundaries among classes, while the LDA uses nonrecursive training to produce linear boundaries. In previous studies, the ANN was successfully used for transient EMG PR [7]. The simple LDA was reported as having comparable classification performance to more complex types [20]–[22] and as being computationally efficient for real-time myoelectric prosthesis control [8]. The detailed LDA algorithm can be found elsewhere [15].

To test the ANN classifier, a fully connected two-layer ANN classifier was built based on the study of Hudgins *et al.* [7]. The network was trained using standard backpropagation. To avoid overfitting, the validation test was used to stop the training iterations [24]. The number of hidden units, which was 10, was experimentally determined based on the criteria described in [7] by using 16-channel EMG data in the Post-HC phase only. The applied learning rate was 0.05 and the momentum parameter was 0.6. These parameters were fixed for all ANN testing.

b) EMG features: EMG features, including autoregression coefficients [25], time-domain features [7], frequency-domain features [26], and time–frequency-domain features [21], [27] have been used in the EMG PR for upper limb prosthesis control. In this study, we selected the auto regression and time-domain features because their computation does not require signal transformation, and therefore, satisfies the requirement of fast time-response. The following features were studied: 1) four time-domain features (TD) (mean absolute value, number of zero crossings, waveform length, and number of slope sign changes [7]); 2) the features with three-order autoregression coefficients and the root mean square of a signal (AR) [25]; and 3) the features combining TD and three-order autoregression coefficients (TDAR).

c) Length of the analysis window: The length of the analysis window for EMG feature extraction was determined by the properties of the signal. The EMG signal was modeled as a wide-sense Gaussian random process [7]. A short analysis window may elicit a large statistical variance of calculated features [8]. The length of analysis window should not exceed 200 ms, within which the contents of EMG signals were assumed to have small variation. Therefore, classification errors resulting from window lengths ranging from 50 to 150 ms were compared.

d) Analysis window increment size: In addition to high classification accuracy, a fast time response is desired for real-time classification. A scheme using overlapping analysis windows was applied in order to generate faster decision updates [8]. The smaller the window increment, the faster the classification decision can be made. We expected to improve the system response time without increasing the classification error.

Analysis of covariance (ANCOVA) was applied to statistically study the effects of EMG features (category variable) and analysis window length (covariate) on classification error. Since the size of the window increment was limited by the analysis window length, the window increment size was studied using one-way analysis of variance (ANOVA) with a fixed window length and feature set.

4) Comparing Classification Error Using Different Amounts of Neuromuscular Control Content—First, the neuromuscular control content was manipulated by selecting different subsets of EMG channels recorded from the able-bodied subjects. For example, to simulate a TF amputee, the EMG channels recording from below-knee muscles were removed from the system input. The purpose of comparing the classification performance using different combinations of EMG electrodes was twofold: 1) to identify the importance of the neuromuscular control information from different muscle groups for accurate classification and 2) to quantify the robustness of the designed system with different amounts of neural control information. Four combinations of EMG channels were studied, as listed in Table I. Combination 1 included all recorded EMG channels; combination 2 contained EMG channels placed above the knee joint; combination 3 incorporated EMG signals recorded from muscles in the thigh only; combination 4 was composed of EMG signals from muscles in the calf and foot.

To further evaluate the phase-dependent design for lower limb prosthesis control, we conducted a pilot investigation on two TF amputees. The pilot study was specifically intended to determine the amount of neural control information contained in EMG signals recorded from the residual limbs of the TF amputees. The classification error derived when using EMG signals from the hip and residual limb was compared to the error derived when using EMG signals recorded from the residual limb only.

III. Results

A. Influence of Design Parameters on Classifier Performance

The classification performance of the LDA and the ANN classifiers was compared (see Fig. 2). For all four studied phases, the LDA produced lower classification error; however, this difference was not statistically significant ($P > 0.05$). If the EMG signals from the whole stride cycle were used as inputs, both methods failed to classify the movement modes correctly; a significantly higher error was observed than that derived from using the EMG signals from short gait phases. Since the LDA classifier is easier to implement without considering parameter regularization, provides lower classification error, and is more computationally efficient than the ANN, the LDA classifier was adopted in the rest of this study.

Fig. 3 shows the influence of analysis window length and EMG features on classification error when the LDA algorithm was used to classify 16 channels of EMG data with a 30-ms window increment. The average errors over able-bodied subjects and all applied features dropped 5.0%–7.1% in all four phases when the window length was increased from 50 to 120 ms, but remained relatively constant when the window length was increased from 120 to 150 ms. The window length significantly influenced the classification errors ($P < 0.05$) in all four phases; the influence of the feature sets reached a significant level ($P < 0.05$) only in the Pre-TO phase. Additionally, in the Pre-TO phase, all three EMG feature sets were compared to one another by the Bonferroni *post hoc* test; the TDAR feature set produced significantly higher errors than the AR feature set ($P = 0.011$) and no significant difference was observed for the other two pairs.

To demonstrate the influence of window increment size on the classifier's performance, window increments from 10 to 60 ms were studied with the window length set to 140 ms and using TD features. A smaller window increment provided slightly lower errors in the four studied phases (see Fig. 4). However, this difference was not statistically significant ($P > 0.05$, one-way ANOVA).

B. Classification Error Using Different Neuromuscular Control Information

Fig. 5 demonstrates the average classification errors over eight able-bodied subjects when different combinations of EMG signals were used as input to the designed PR system. Impressively, when EMG signals from muscles in the hip and thigh were used (combination 2), the classification errors in the four defined phases were $12.4\% \pm 5.0\%$, $6.0\% \pm 4.7\%$, $7.5\% \pm 5.1\%$, and $5.2\% \pm 3.7\%$ (dark gray bars in Fig. 5). Adding EMG signals from distal muscles reduced the errors by 1.8%–3.0% (black bars in Fig. 5), and removing two gluteal muscles increased the errors by 0.2%–2.8% (light gray bars in Fig. 5); however, none of these changes were statistically significant ($P > 0.05$, one-way ANOVA). Finally, among all EMG signal combinations, the combination including EMG signals from the shank and foot produced the highest classification errors (white bars in Fig. 5).

Fig. 6 shows the error in identifying each individual task as the result of using the data collected from the two amputee subjects. When EMG signals from the gluteal and thigh muscles were used (black bars in Fig. 6), the overall classification errors (CE) in the Post-HC, Pre-TO, Post-TO, and Pre-HC phases were 15.2%, 8.6%, 5.2%, and 3.8% for TF1 and 12.4%, 11.9%, 3.8%, and 7.1% for TF2, comparable to the results derived from able-bodied subjects. When using EMG signals from muscles in the residual limb only, the overall errors in the four phases were increased to 19.0%, 19.0%, 8.6%, and 6.7% for TF1 and 22.9%, 17.1%, 8.5% and 12.9% for TF2.

C. Phase-Dependent Classification Error

The classification error was phase-dependent. The confusion matrices averaged over eight able-bodied subjects as a result of using the EMG channels above the knee (combination 2) in four gait phases are shown in Fig. 7. Each element in the matrix is represented by a bar, the height of which maps the value of the element. The numbers above the diagonal elements are the average classification accuracies for identifying individual tasks. The lowest classification accuracy occurred in the Post-HC phase among the tasks of level-ground walking, stepping over an obstacle, and turning. The stair ascent and descent tasks were the most robustly recognized locomotion modes in all studied phases; the average classification accuracy of these two modes ranged from 93.8% to 99.3%. None of the locomotion modes were confused with the task of standing still. A similar result was also observed for the TF amputee subjects (black bars in Fig. 6).

IV. Discussion

This study demonstrates that the designed phase-dependent EMG PR system was able to accurately recognize seven task modes when sufficient neural control information was present in the input EMG signals, while applying PR to an entire stride could not provide reliable classification with the time-varying EMG input. This supports our design concept that nonstationary EMG signals recorded during locomotion could be modeled as stationary within a short time window.

Perhaps the most exciting result was the similar classification error between using EMG combination 2 (Table I) recorded from the able-bodied subjects (dark gray bars in Fig. 5) and EMG signals of the amputee subjects (black bars in Fig. 6). In both cases, the input EMG signals were recorded from the gluteal and thigh muscles only. The results of this preliminary testing suggest that sufficient neural control information for accurate classification of various locomotion modes can be extracted from EMG signals recorded from muscles above the knee in able-bodied subjects and possibly individuals with long TF amputations. Although the two participating amputee subjects have had TF amputations for more than 30 years, our study demonstrated that the muscles in their residual limbs still modulated with consistent activation patterns. The amputees' EMG patterns did not necessarily follow the patterns of able-bodied subjects; however, since EMG PR algorithms adapt to each individual, our designed phase-dependent EMG PR strategy was able to provide relatively high classification accuracy with the amputee subjects as well.

Removing the EMG signal input from the hip muscles slightly increased the classification error for the able-bodied subjects (light gray bars in Fig. 5), while for the amputee subjects, the hip muscles were more important for improving the mode identification accuracy during stance phase. This may be because the hip muscles become more important for stabilizing the lower limb during walking for amputee patients. Unfortunately, it may be difficult in practice to record the EMG signals of hip muscles using a prosthetic socket.

The electrode information from below the knee represents data that could possibly be made available with targeted muscle reinnervation. The increase in accuracy was modest in the able-bodied subjects with this control scheme. This suggests that TMR may not be needed with this control scheme for long TF amputees. However, TMR may improve the classification accuracy if hip muscle EMG is not used in the long TF amputee, and it is likely that TMR can be useful for patients with short TF or higher levels of amputations. When the recordable neuromuscular control information is highly limited, TMR could allow neural control data to be accessible for the lower amputated leg muscles, and therefore, enhance mode selection. In addition, TMR might be feasible for other EMG-based prosthesis control paradigms. For example, we could restore a dorsiflexion signal from a common peroneal nerve transfer or a plantar flexion signal from a tibial nerve transfer. These signals could be used consciously for mode selection: a strong voluntary dorsiflexion signal may be used to put the prosthesis into a stair climbing mode and a strong plantar flexion signal may be used to put the leg into a stair descending mode. Finally, TMR may be of value for multiarticular control of powered leg prostheses.

Not surprisingly, the mode selection error rates were higher when recording only from muscles below the knee (as with transtibial amputation) with these tasks. Knee and hip EMG signals clearly added more information to identify the subject's mode of movement.

The accuracy in recognizing locomotion modes also depends on the gait phase and the investigated tasks. The Post-HC phase is the very beginning of the transition between the level-ground walking task and other tasks; the difference in EMG patterns among the tasks of level-ground walking, stepping over an obstacle, and turning was subtle; the classifier

could not separate these locomotion modes as clearly (see Figs. 6 and 7). An accurate decision before toe-off and heel contact is important for assuring safety, because the controller could decide the motion of the prosthetic knee before the execution of the swing and the next weight acceptance. Impressively, the high risk activities of stair ascent and descent were the most easily identified among the studied tasks; this is perhaps because these two tasks had significantly different kinematics and kinetics, and involved more voluntary drive (attention) from the user.

Based on the results of our study, the following variable designs are recommended in order to build a robust EMG pattern classifier for identifying user locomotion modes: 1) the LDA and the ANN provided comparable classification performance in the phase-dependent PR system; however, the LDA is preferred because it is fast to train, easy to design, and computationally efficient for real-time prosthesis control. For the ANN, the complexity of the classifier may need to be adjusted if parameters such as the number of applied EMG channels, the patterns to be learned, and the number of classes are changed. The poor generalization capability of ANN challenges its clinical application for prosthesis control; 2) TD and AR features are computationally efficient and provide similar classification accuracies compared to TDAR features; TD and AR features are preferred; 3) Analysis window lengths greater than 120 ms are desirable (see Fig. 3). This result is consistent with the outcomes of several previous studies [8], [20], but is opposite to the result reported by Hudgins *et al.* [7], who reasoned that a shorter analysis window could better capture the features of deterministic signal components, which were found in the studied transient EMG signals and were considered motion artifacts. In our study, the slow wave and motion artifacts were filtered out, resulting in a different outcome; 4) A small increment permits fast decision updates without influencing the classification error. Nevertheless, the minimum increment size must be limited by the processing delay, which consists of the time required to compute the feature vector and discriminate the data [8] and depends on the applied hardware system. These recommendations are made within the limitations of this preliminary study. Further studies aimed at optimizing the nonstationary EMG PR design, such as those looking at other types of classifiers, at EMG features other than TD and AR, and at the feature selection method will be necessary.

Although the classification accuracies found in this study are encouraging, they are clearly not sufficient to be used independently for a prosthetic leg control system. Additional technology will be required for future clinical implementation. One promising technique, called multisensor fusion, enhances machine perception and PR accuracy by sensing multiple sources of data rather than a single source [28]. By basing class decisions not only on EMG data but also on peripheral sensing data, such as ground reaction forces and joint kinematics monitored from the prosthesis, the active prosthetic controller might further improve the classification accuracy. Additionally, the turning tasks, heavily confused with each other and the level-ground walking task, may be eliminated from the selected modes for better classification accuracy; amputee subjects were able to perform the turning tasks safely using passive devices with the level-walking control mode. Furthermore, the control safety could be further reinforced by using the already existing safety mechanisms achieved in current leg systems. This study also highlights many other development issues. Due to the lack of monitored gait events from the other limb, the applied phases were not clinically defined, and results in the midstance phase were missing [see Fig. 1(b)]. Additionally, the constant length of the phase window (200 ms) is inappropriate for a task with a short stride cycle or for a person with fast cadence. Since muscle activity is directly related to the dynamic control of each gait phase, the classifiers may need to be built corresponding to clinically and functionally defined phases. This study is only the first step in investigating if EMG could be used for neural prosthesis control. Furthermore, the testing on two subjects with TF amputations can only be considered case studies. Additional efforts are needed,

including testing more subjects with various levels of TF amputations, developing a real-time gait phase detection module, and designing a safe and robust prosthesis control system including data from sensors in the prosthesis.

V. Conclusion

This study demonstrates an initial attempt to develop and evaluate a phase-dependent EMG PR algorithm for identifying locomotion modes. The results of this pilot study suggest that the concept of phase-dependent PR design is viable for the design of neural-controlled prosthetic legs. However, continuing efforts will be required to further improve the EMG PR design, include other activities of daily living, and make the accuracy of recognizing the user's movement mode acceptable for safe and robust prosthetic control.

Acknowledgments

This work was supported in part by the Globe Foundation, in part by the National Institutes of Health (NIH) National Institute of Child and Human Development under Grant R01 HD043137, and in part by the National Institute on Disability and Rehabilitation Research, U.S. Department of Education, under Grant H133F080006.

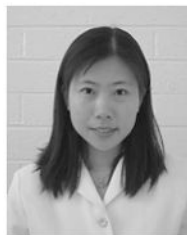
We would like to thank K. Englehart, Ph.D., at the University of New Brunswick, G. Li, Ph.D., and J. Sensinger, Ph.D., for assistance with this manuscript. We thank A. Schultz, M.S., for editing the manuscript.

References

1. Psonak, R. Transfemoral prosthetics. In: Lusardi, MM.; Nielsen, CC., editors. *Orthotics and Prosthetics in Rehabilitation*. Boston, MA: Butterworth-Heinemann Publications; 2000.
2. Johansson JL, Sherrill DM, Riley PO, Bonato P, Herr H. A clinical comparison of variable-damping and mechanically passive prosthetic knee devices. *Amer J Phys Med Rehabil* 2005;84:563–575. [PubMed: 16034225]
3. Peeraer L, Aeyels B, Van Der Perre G. Development of EMG-based mode and intent recognition algorithms for a computer-controlled above-knee prosthesis. *J Biomed Eng* 1990;12:178–182. [PubMed: 2348704]
4. Herr H, Wilkenfeld A. User-adaptive control of a magnetorheological prosthetic knee. *Ind Robot: Int J* 2003;30:42–55.
5. Williams TW III. Practical methods for controlling powered upper-extremity prostheses. *Assist Technol* 1990;2:3–18. [PubMed: 10149040]
6. Parker PA, Scott RN. Myoelectric control of prostheses. *Crit Rev Biomed Eng* 1986;13:283–310. [PubMed: 3512166]
7. Hudgins B, Parker P, Scott RN. A new strategy for multifunction myoelectric control. *IEEE Trans Biomed Eng* Jan;1993 40(1):82–94. [PubMed: 8468080]
8. Englehart K, Hudgins B. A robust, real-time control scheme for multifunction myoelectric control. *IEEE Trans Biomed Eng* Jul;2003 50(7):848–854. [PubMed: 12848352]
9. Horn GW. Electro-control: An EMG-controlled A-K prosthesis. *Med Biol Eng* 1972;10:61–73. [PubMed: 5044871]
10. Saxena SC, Mukhopadhyay P. E.M.G. operated electronic artificial-leg controller. *Med Biol Eng Comput* 1977;15:553–557. [PubMed: 199811]
11. Jin D, Yang J, Zhang R, Wang R, Zhang J. Terrain identification for prosthetic knees based on electromyographic signal features. *Tsinghua Sci Technol* 2006;11:74–79.
12. Kuiken TA, Miller LA, Lipschutz RD, Lock BA, Stubblefield K, Marasco PD, Zhou P, Dumanian GA. Targeted reinnervation for enhanced prosthetic arm function in a woman with a proximal amputation: A case study. *Lancet* 2007;369:371–380. [PubMed: 17276777]
13. Kuiken TA, Dumanian GA, Lipschutz RD, Miller LA, Stubblefield KA. The use of targeted muscle reinnervation for improved myoelectric prosthesis control in a bilateral shoulder disarticulation amputee. *Prosthet Orthot Int* 2004;28:245–253. [PubMed: 15658637]

14. Zhou P, Lowery MM, Englehart KB, Huang H, Li G, Hargrove L, Dewald JP, Kuiken TA. Decoding a new neural-machine interface for control of artificial limbs. *J Neurophysiol* Nov;2007 98(5):2974–2982. [PubMed: 17728391]
15. Huang H, Zhou P, Li G, Kuiken TA. An analysis of EMG electrode configuration for targeted muscle reinnervation based neural machine interface. *IEEE Trans Neural Syst Rehabil Eng* Feb; 2008 16(1):37–45. [PubMed: 18303804]
16. Delagi, EF.; Perotto, A. *The Limbs. 2.* Springfield, IL: Thomas; 1980. *Anatomic Guide for the Electromyographer*—.
17. Hase K, Stein RB. Turning strategies during human walking. *J Neurophysiol* 1999;81:2914–2922. [PubMed: 10368408]
18. Frey, BJ. *Graphical Models for Machine Learning and Digital Communication.* Cambridge, MA: MIT Press; 1998.
19. Micera S, Sabatini AM, Dario P, Rossi B. A hybrid approach to EMG pattern analysis for classification of arm movements using statistical and fuzzy techniques. *Med Eng Phys* 1999;21:303–311. [PubMed: 10576421]
20. Huang Y, Englehart KB, Hudgins B, Chan AD. A Gaussian mixture model based classification scheme for myoelectric control of powered upper limb prostheses. *IEEE Trans Biomed Eng* Nov; 2005 52(11):1801–1811. [PubMed: 16285383]
21. Englehart K, Hudgins B, Parker PA, Stevenson M. Classification of the myoelectric signal using time-frequency based representations. *Med Eng Phys* 1999;21:431–438. [PubMed: 10624739]
22. Hargrove LJ, Englehart K, Hudgins B. A comparison of surface and intramuscular myoelectric signal classification. *IEEE Trans Biomed Eng* May;2007 54(5):847–853. [PubMed: 17518281]
23. Sebelius FC, Rosen BN, Lundborg GN. Refined myoelectric control in below-elbow amputees using artificial neural networks and a data glove. *J Hand Surg [Amer]* 2005;30:780–789.
24. Duda, RO.; Hart, PE.; Stork, DG. *Pattern Classification. 2.* New York: Wiley; 2001.
25. Graupe D, Salahi J, Kohn KH. Multifunctional prosthesis and orthosis control via microcomputer identification of temporal pattern differences in single-site myoelectric signals. *J Biomed Eng* 1982;4:17–22. [PubMed: 7078136]
26. Peleg D, Braiman E, Yom-Tov E, Inbar GF. Classification of finger activation for use in a robotic prosthesis arm. *IEEE Trans Neural Syst Rehabil Eng* Dec;2002 10(4):290–293. [PubMed: 12611366]
27. Boostani R, Moradi MH. Evaluation of the forearm EMG signal features for the control of a prosthetic hand. *Physiol Meas* 2003;24:309–319. [PubMed: 12812417]
28. Hall D, Llinas J. An introduction to multisensor data fusion. *Proc IEEE* Jan;1997 85(1):6–23.

Biographies



He Huang (M'06) received the B.S. degree in bio-electronics engineering from Xi'an Jiao-Tong University, Xi'an, China, in 2000, and the M.S. and Ph.D. degrees in bioengineering from Arizona State University, Tempe, in 2002 and 2006, respectively.

She completed her post-doc training in the Neural Engineering Center for Artificial Limbs, Rehabilitation Institute of Chicago. She is currently an Assistant Professor in the Department of Electrical, Computer, and Biomedical Engineering, University of Rhode Island. Her research interests include neural-machine interface, modeling and analysis of

neuromuscular control of movement in normal and neurologically disordered humans, virtual reality in neuromotor rehabilitation, and design and control of therapeutic robots, orthoses, and prostheses.



Todd A. Kuiken (M'99–SM'07) received the B.S. degree in biomedical engineering from Duke University, Durham, NC, in 1983, and the Ph.D. degree in biomedical engineering and the M.D. degree from Northwestern University, Chicago, IL, in 1989 and 1990, respectively.

In 1995, he completed the Residency in Physical Medicine and Rehabilitation at the Rehabilitation Institute of Chicago and Northwestern University Medical School, Chicago. He is currently the Director in the Neural Engineering Center for Artificial Limbs, Rehabilitation Institute of Chicago, Chicago, where he is also the Director of Amputee Services, and the Associate Dean for Academic Affairs in the Feinberg School of Medicine. He is also an Associate Professor in the Departments of Physical medicine and rehabilitation (PM&R) and Biomedical Engineering, Northwestern University.



Robert D. Lipschutz received the B.Sc. degree in mechanical engineering from Drexel University, Philadelphia, PA, in 1988, and the Certificate in prosthetics and orthotics from the Post Graduate Medical School, New York University, New York, in 1990.

He completed his prosthetics training at the Shriner's Hospital for Crippled Children, Springfield, MA, and continued his clinical endeavors at Newington Children's Hospital, Newington, CT. He is currently a Research Prosthetist in the Neural Engineering Center for Artificial Limbs, Rehabilitation Institute of Chicago, Chicago, IL. His current research interests include fitting and evaluation of new advanced prosthetic devices.

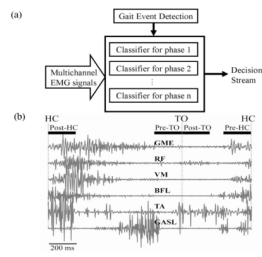


Fig. 1.

(a) Architecture of phase-dependent EMG pattern classifier. (b) Four defined phase windows aligned with heel contact (HC) and toe-off (TO). Raw EMG signals in one stride cycle are demonstrated.

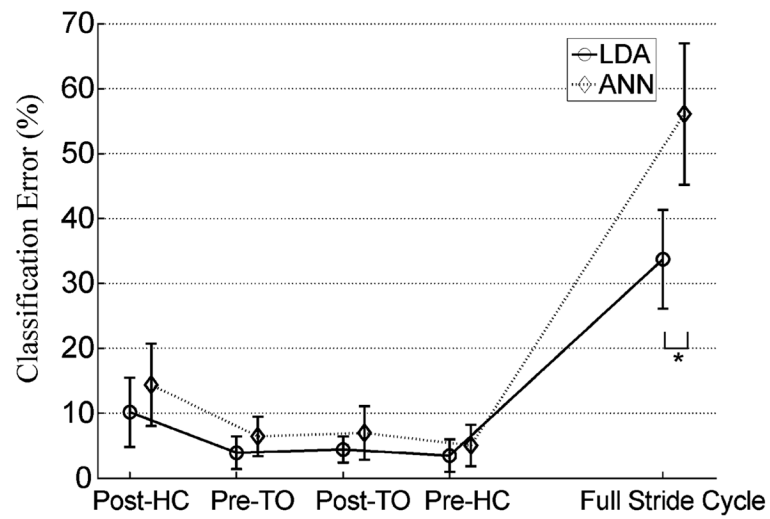


Fig. 2. Classification performance of the LDA and the ANN classifiers. The classification errors were averaged over eight able-bodied subjects. The results derived from the phase-dependent PR and the full-stride PR design are demonstrated. * demonstrates statistically significant difference (one-way ANOVA, $P < 0.05$). In this test, the TD features, 16 EMG channels, 140-ms windows, and 30-ms window increments were used.

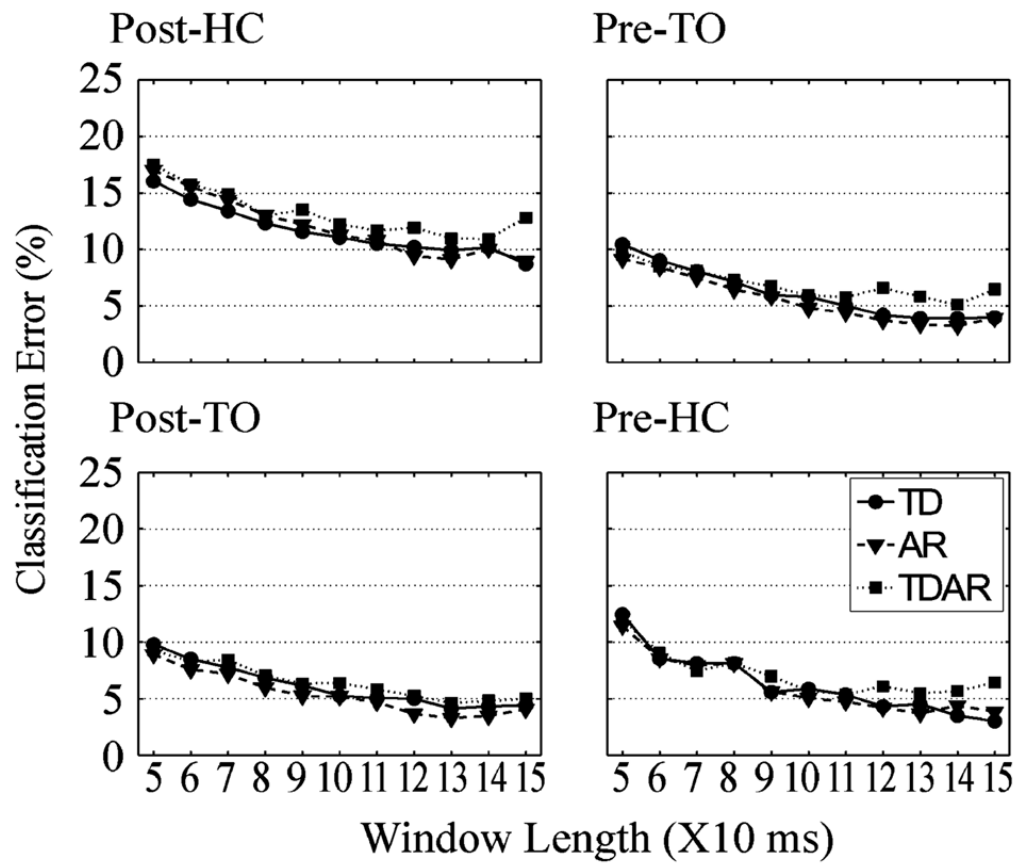


Fig. 3. Influence of EMG features and length of the windows on classification error of LDA. The averaged classification error over eight subjects is demonstrated in each defined gait phase. The size of the window increment was set to 30 ms.

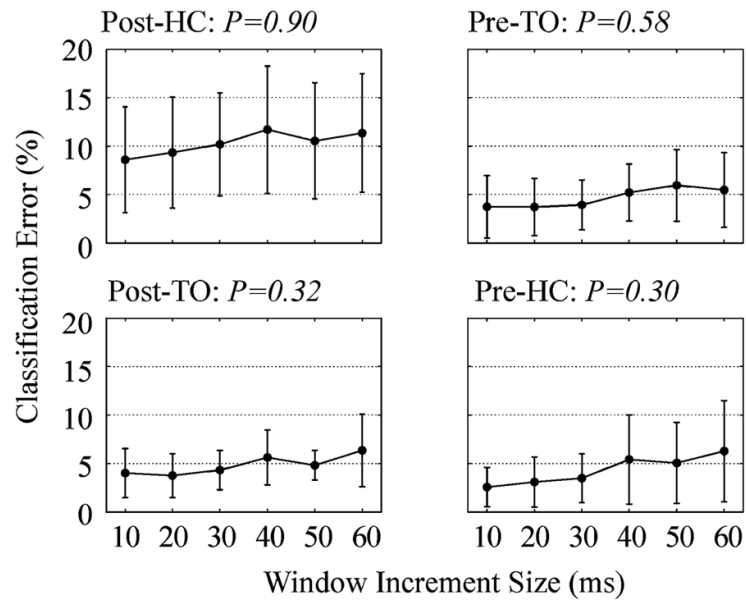


Fig. 4. Influence of window increment size on classification error. The error averaged over eight subjects is shown in each defined gait phase. A 140-ms analysis window and TD EMG features were applied. The P -values derived from a one-way ANOVA are presented above individual phases.

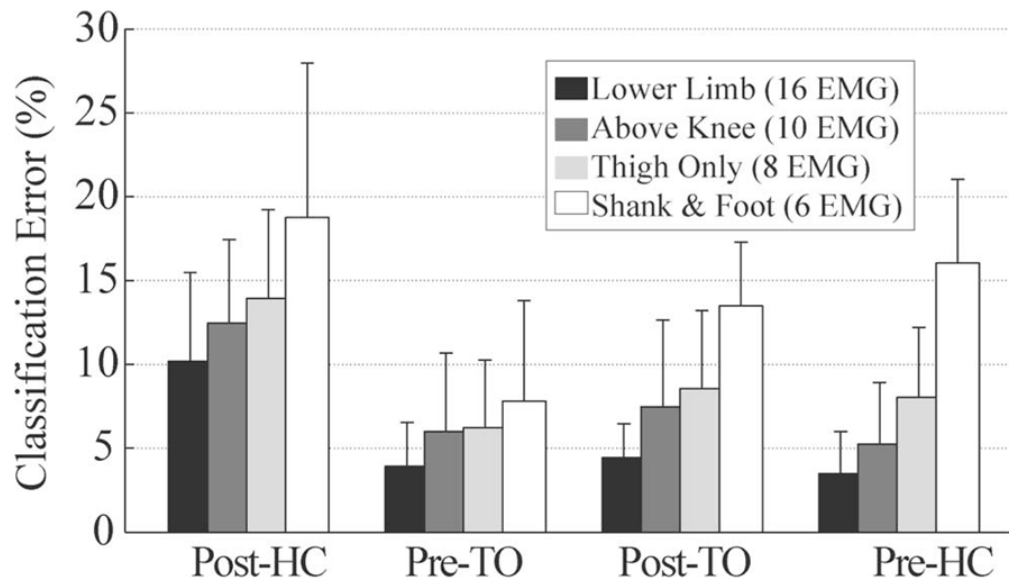


Fig. 5. Comparison of classification error averaged over eight able-bodied subjects using different amounts of neuromuscular control information. Combination 1 (black bars): the classification error found using all recorded 16 EMG channels; combination 2 (dark gray bar): the error found using 10 EMG channels above the knee; combination 3 (light gray bars): the error found using EMG of thigh muscles only; combination 4 (white bars): the error found using EMG from muscles in shank and foot.

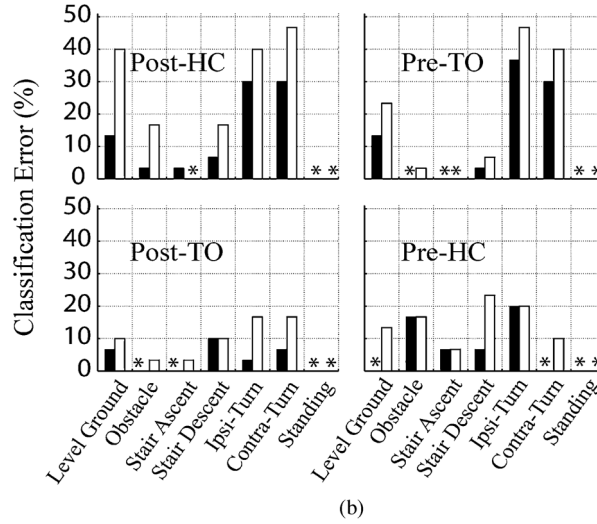
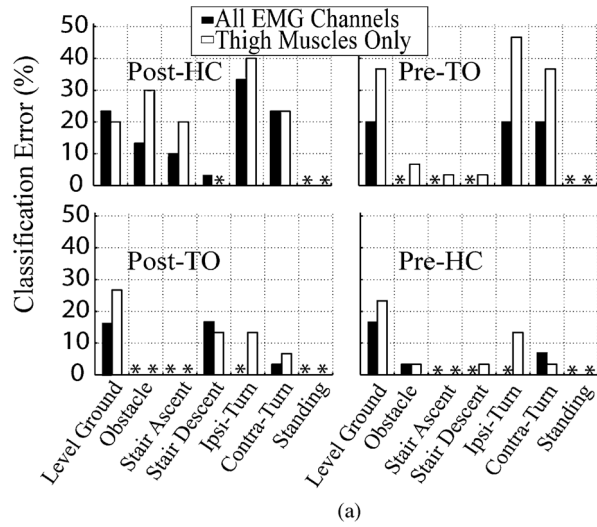


Fig. 6. Classification error of each task mode for data recorded from subjects (a) TF1 and (b) TF2. (Black bars) Classification error of each task found using all 11 channels of EMG. (White bars) Classification error of each task found using EMG signals in the residual limb only (nine channels). * denotes 0% classification error.

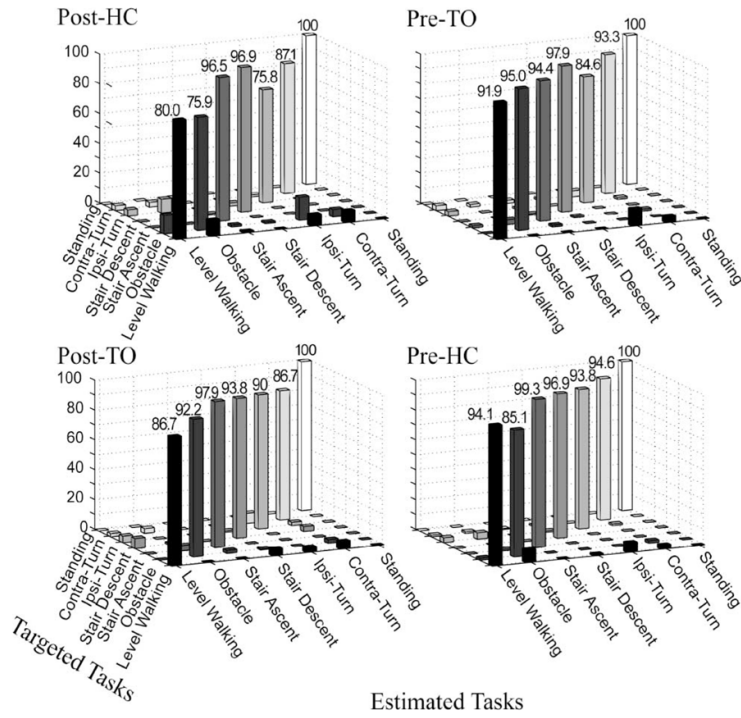


Fig. 7. Bar chart of the confusion matrix for mode classification averaged over eight able-bodied subjects in each phase using EMG from ten muscles above the knee. TD features, 140-ms window length, and 30-ms window increments were used. At the interception of the estimated task j and the targeted task i , a bar is demonstrated, and its height maps the value of element in the confusion matrix. The diagonal values of the matrix, representing the average classification accuracy rate for individual tasks, are shown above the diagonal bars.

Table I

Studied Combinations of EMG Channels in Eight Able-Bodied Subjects

	EMG Channels			
	Pelvis Segment	Thigh Segment	Calf Segment	Foot Segment
	GMA, GME	SAR, RF, VL, VM, GRA, BFL, SEM, BFS	TA, PL, GASL, GASM, SOL	EDB
1	Included	Included	Included	Included
2	Included	Included	--	--
3	--	Included	--	--
4	--	--	Included	Included